Pakistan Veterinary Journal

ISSN: 0253-8318 (PRINT), 2074-7764 (ONLINE)
DOI: 10.29261/pakvetj/2023.037

RESEARCH ARTICLE

Anatomical and Histopathological Comparative Studies Between Right and Left Mammary Tumors in a Rat Model Induced by DMBA

Nali A. Maaruf*, Suhail M. Najjar and Salah A. Ali

Department of Anatomy and Pathology, College of Medicine, Hawler Medical University 4601, KRG/Iraq
*Corresponding author: nali.maaruf@hmu.edu.krd; nalimaaruf@gmail.com

ARTICLE HISTORY (23-052)

Received: January 25, 2023
Revised: May 8, 2023
Accepted: May 15, 2023
Published online: May 29, 2023

Key words:
DMBA
HER2
Fibroadenoma
Invasive ductal carcinoma
Lobular carcinoma in situ
Ki67

A B S T R A C T

Breast carcinoma is the second most common type of cancer in women, and its progress and outcome depend on the expression of the human epidermal growth factor receptor 2 (HER2), progesterone receptor (PR), estrogen receptor (ER), and Ki67 genes. This research evaluated morphological, histological, and immunohistochemical markers, including ER, PR, Ki67 and HER2 expression differences between right and left mammary tumors. Two hundred, 7-week-old virgin female Sprague Dawley rats, weighing 100–120g were used in the study. The rats were divided into two groups: G1 = control negative (n = 50), which received just a placebo (normal saline), and G2 = control positive (n = 150), which received a single dose of 20 mg/kg body weight of DMBA by gavage after being dissolved in sesamoid oil. Animals were weighed and monitored weekly until the end of the study. On week 16, a lumPwas taken from the right and left mammary glands and examined by hematoxylin-eosin staining and immunohistochemistry (IHC) using ER, PR, HER2 and Ki67 antibodies. Out of the 150 total numbers, 87 tumors were induced by DMBA; 44.83% (39/150) appeared on the right mammary gland chain and 49.43% (43/150) on the left, and most of the tumors were found on cervical-thoracic glands. ER, PR and Ki67 expression were higher than HER2 in all tumors. We found that the histopathological features of mammary cancer in rats induced by DMBA were similar to those of human breast cancers in terms of location, histopathologic alterations, and IHC markers, and location plays a significant role in tumor development and IHC susceptibility.

To Cite This Article: Maaruf NA, Najjar SM and Ali SA, 2023. Anatomical and histopathological comparative studies between right and left mammary tumors in a rat model induced by DMBA. Pak Vet J, 43(2): 232-240. http://dx.doi.org/10.29261/pakvetj/2023.037

INTRODUCTION

The differences between right and left-sided breast cancer (BC) are not well understood. A few studies have been conducted on lateral differences and the frequency of BC; studies on the morphological differences between right and left-sided BC are also rare. BC in women is more likely to develoPon the left side than the right, with ratios ranging from 1.05 to 1.26. The difference is not big, but it's also not thought to be small (Cheng *et al*., 2018).

BC is the second-most common malignancy and the second-leading cause of death in female patients worldwide (Siddarth *et al*., 2016). It is diverse cancer with a variety of histological classifications, as well as molecular and clinical characteristics (Vedashree and Rajalakshmi, 2016). The most valuable factors in assessing prognosis are the histomorphological type, tumor diameter, tumor necrosis, invasion of the skin, nipple and chest wall, lymphovascular invasion, a grade with stage, estrogen receptor (ER) status, progesterone receptor (PR), human epidermal growth factor receptor 2 (HER2), cell proliferation marker (ki-67) and therapy regimen (Asif *et al*., 2014; Dong *et al*., 2018).

Due to its prevalence, scientists have tried to detect and treat this disease earlier. As a result, numerous research teams have worked to create experimental models of mammary carcinogenesis to better understand its different phases and make advancements in cancer prevention and treatment. Numerous radiation carcinogenesis models (Wincewicz *et al*., 2010) and chemical carcinogens (Cheung *et al*., 2011), as well as methods for inducing the development of tumors utilizing various doses, have been presented. The most prevalent carcinogens include 7,12-dimethylbenz[a]-anthracene (DMBA) (De Oliveira *et al*., 2015).

7,12-dimethylbenz(a)anthracene (DMBA), one of the carcinogenic polycyclic aromatic hydrocarbons that are used to cause breast cancer, is converted into DMBA-3,4-diol-1,2-epoxide (DMBA-DE), which disrupts tissue redox

equilibrium and causes oxidative stress. Reactive oxygen species that come from this damaged DNA or a protein cell cycle, can cause unregulated cell division and growth (Sung *et al*., 2021).

The most effective prognostic indicator for BC is the expression of the estrogen (ER) and progesterone receptors (PR) (Vedashree and Rajalakshmi, 2016), which are intercellular steroid hormone receptors found on the surface of normal and cancerous breast cells. These receptors are activated by the hormones estrogen and progesterone, respectively. Once activated, ER and PR can promote cell growth and division, which can lead to the development of breast cancer (Nabi *et al*., 2016). In breast cancer, ER and PR can be present at varying levels. high levels of ER or PR are known as hormone receptor-positive (HR-positive which tend to be less aggressive and more responsive to hormone therapy than hormone receptor-negative cancers (Shah *et al*., 2016). However, if a tumor spreads to form metastases, ER and PR status may alter. A worse prognosis is linked to an ER or PR condition going from positive to negative (Meng *et al*., 2016).

Besides hormone receptors, HER2 is a potential BC biomarker, and it has a crucial role in the etiology of several human malignancies, it is played by the human epidermal growth factor receptor (HER) family of receptors. They regulate cellular proliferation, differentiation, growth, survival, and differentiation via signal transduction pathways. About 18-20% of breast tumors overexpress HER2-, which is predictive and prognostic of a poor prognosis (Singh *et al*., 2019).

Since the 1980s, Ki67 has been recognized as a significant proliferation biomarker. Along with ER, PR, and HER2, it is now a crucial part of the regular biomarker profile for BC, which helps oncologists treat BC patients as effectively as possible. Numerous studies have revealed a substantial association between Ki67 positivity and histology markers such as nuclear grades and mitotic figures, supporting its very well position as a poor prognostic biomarker (Taneja *et al*., 2010). Ki67 positivity is strongly associated with histology markers such as nuclear grades and mitotic figures, which confirms its role as a poor prognostic biomarker. This hypothesis is supported by numerous studies that have demonstrated a significant correlation between Ki67 expression and aggressive tumor behavior, including higher tumor grade, increased proliferation rate, and poor clinical outcomes (Davey *et al*., 2021).

The present study is designed to determine any differences in the morphological (gross anatomy) and histopathological changes between right and left mammary cancer and to investigate the expression patterns of the clinically most critical molecules for mammary cancer (ER, PR, HER2 and Ki-67) by immunohistochemical (IHC) analysis. This study provides a key to resolving higher liability of the left breast than the right for carcinoma even by very limited frequency, which can be used as a matter to decrease the BC incidences in the future bilaterally.

MATERIALS AND METHODS

Animals: Two hundred virgin female Sprague-Dawley (SD) rats, six seven weeks old and weighing 100-120 g, were obtained from the Animal House, College of Pharmacy, and Hawler Medical University for this study. They were maintained in cages with a 12-hour light/12-hour darkness cycle and ad libitum food and water. During the study, the specifications proposed by guidelines for the welfare and use of animals in university lab center research were followed as suggested by Bülbül and Nawaz (2020) The female Sprague-Dawley rats were allocated into two groups: G1 = control negative (n = 50), in which rats were treated only with normal saline and G2 = control positive (n = 150), in which rats were treated with 7,12-dimethylbenzanthracene (DMBA).

Ethical approval: This study was approved by the Research Ethics Committee and Institutional Animal Care of the Hawler Medical University, College of Medicine Kurdistan/Iraq, ID (HMU 4,2) ethical norms for animal experimentation.

Study design: The carcinogen DMBA was obtained in powder form (Sigma-Aldrich, USA); before its use, DMBA was diluted in sesamoid oil and mixed well by using a vortex mixer (1000 mg of DMBA and 50 ml of Sesamoid oil). At age 7 weeks, rats in the control positive grouP(G2) were given a single dose of DMBA (20 mg/kg body weight) orally using gavage (Barros *et al*., 2004) with modification.

Each rat has six pairs of mammary glands that are divided into two groups; the first group: three pairs in the pectoral region (cervicothoracic region), and the second group: Three pairs in the inguinoabdominal region.

After 7 weeks of DMBA administration, all rats were observed daily for their clinical status. The weight of the rats was measured weekly throughout the experimental period. Palpation for all mammary glands in each region was done twice a week to detect any growth, and visible tumor nodules were measured using vernier calipers at regular intervals; then microscopic examinations were performed for the nodule or lumPweekly after preparing the histologic section. Mortality was recorded until the end of the experiment (Barros *et al*., 2004) with modification.

Histology and immunohistochemical analysis: At the end of the experiment (16 weeks after the administration of DMBA), the rats were sacrificed. The lumps from both the right and left mammary glands were excised. Neoplastic tissues were fixed overnight in 10% neutral buffered formalin (NBF) for microscopy and immunohistochemistry (Hassan *et al*., 2022). Tissues were processed for paraffin infiltration and embedding. Five sections of 4 µm from each region were mounted on normal and charged microscope slides (Fisher Scientific, PA). To identify tumor types, a light microscopic (Leica, Germany) examination of serial Hematoxylin and eosin (H&E)-stained sections representative of a given tumor was performed, followed by photomicrographing (AmScope™, China) at 100X and 400X magnification.

For immunohistochemistry, sections were dewaxed in xylene, rehydrated through graded ethanol concentrations, then rinsed in distilled water. Sections were subjected to the heat-induced epitope retrieval method in 10 mmol/L citrate buffer (pH 6.0) for PR and ER. For Ki-67 antigen retrieval, edetic acid and ethylenediaminetetraacetic acid (EDTA) retrieval solution at pH 9 was used, and for HER2 heat-

induced epitope retrieval, 10 mM citric acid monohydrate (pH 6.0) was used. All sections were then heated in a standard microwave oven for 20 minutes. Endogenous peroxidase activity was blocked with 3% hydrogen peroxide (Dako, Denmark) for 10 minutes. The first sections were incubated with the primary antibody anti-Ki67 (1:600 dilution, Dako, Denmark catalog number: IR626) for 30 minutes at 25°C according to the manufacturer's instructions. Two sections were incubated for 60 minutes at room temperature with each of the following polyclonal antibodies: rabbit anti-PR polyclonal antibody (1:600 dilution, DAKO, Denmark catalog number: IR068), rabbit anti-ER-a polyclonal antibody (1:300 dilution, DAKO, Denmark catalog number: IR084). The last section was incubated for 60 minutes at room temperature with an anti-HER2 polyclonal antibody (1:600 dilution, DAKO, Denmark catalog number: K5731). Sections were then washed and sequentially incubated with a secondary antibody (biotinylated goat anti-rabbit IgG (DAKO, Denmark catalog number: P0449) and a streptavidin-linked horseradish peroxidase product for 30 minutes at room temperature. Bound antibodies were visualized following incubation with 3,3-diaminobenzidine (DAB) solution (DAKO, Denmark) for 5 minutes. Sections were counterstained with Meyer's hematoxylin, dehydrated, cleared, and mounted for microscopic examination. The protocol adopted by (Nawaz, 2020 and Akkaya *et al*., 2022) with some modifications

For ER, PR, Ki-67 and HER2, the outcomes were graded independently by three pathologists/investigators. The proportion of tumor cells that stained favorably (in the range of 0% to 100%) was used to quantify the outcome. The percentage of positive cells was calculated as follows: 0 = no positive cells; 1 = 1-10%; 2 = 11-25%; 3 = 26-50%; and 4 = 51-75% positive cells. The average staining intensity was also graded as 0 = negative, 1 = weak, 2 = moderate, or 3 = high. Scores for intensity and proportion were found. To obtain a staining score that ranged from 0 to 12, the degree of positive reactivity and staining intensity were multiplied. Nuclear brown staining was positive for ER, PR, and Ki67, and membranous-cytoplasmic brown staining for HER2 (Singh *et al*., 2019; Al-Nuaimi *et al*., 2020) with modification.

Statistical analysis: An unpaired t-test analysis of variance was used to analyze mammary tumor size and weight following DMBA treatment. Statistical significance was set at $P \leq 0.05$, and all Pvalues were unadjusted for multiple comparisons. Data analyses were generated and plots were constructed using GraphPad Prism 8 (GraphPad Software, Inc., La Jolla, CA, USA).

RESULTS

General observation and measurement of tumors: All rats gained weight until week 10 after DMBA administration, the average body weight of both groups was approximately equal. After week 10, the treated group's body weight dropped, which indicated the tumor's appearance and the ultimate body weight ranged between 235 and 250 g with a 90% survival rate. Control-negative animals gained weight ranging between 300-350 and were tumor-free throughout the study.

A single DMBA used in this study was able to induce breast tumors, which began to appear in the 10^{th}-13^{th} week. However, the vast majority of tumors appeared starting from the 16^{th} week. The lumPwas detected by palpation of both sides of the mammary gland and to observe the lumPall the hair was removed by shaver, then it was removed in each rat using an aseptic procedure under general anesthesia. The mass had a lobulated or discoid pattern with solid or firm consistency that was white to gray or pink. The firm lumps contained necrotic tissue (Fig. 1a-c).

Table 1 revealed the locations and numbers of mammary tumors among different sides of a rat's mammary gland; Out of the 150 total numbers, eighty-seven tumors were induced by DMBA (Table 1), and 44.83% (39/87) appeared on the right mammary gland chain and 49.43% (43/87) occurred on the left mammary gland chain, while 5.75% (5/87) were found in both right-left (bilateral) regions. Region-wise, 45.98% (40/87) of the tumors incidence on abdominal-inguinal mammary glands (45% right, 50% left and 5% bilateral), and 54.02% (47/87) appeared on the cervical thoracic mammary glands (44% right, 48% left and 8% bilateral) with a non-significant difference (Table 2). Tumor sizes were measured from both sides by vernier caliper, also the tumor's weight was taken by sensitive balance and showed variable measurement (Table 2), the significantly bigger sized (25.51 ± 0.8616 and 22.49 ± 0.8355) and heaviest weighted (2.576 ± 0.1288 and 2.186 ± 0.1226) tumor was found in the right and the left sides respectively of the inguinoabdominal region of rat's mammary gland with (P-value =0.004) vs. to the mammary tumor that developed in the cervicothoracic area revealed the smaller sized (23.45 ± 0.9542 and 20.48 ± 0.8623) and lowest weighted (2.272 ± 0.08481 and 1.969 ± 0.08346) in the right and left side respectively with (P-value =0.001). While the mammary gland tumor in the right region was non-significantly bigger and heavier in weight in comparison to the left side in both regions as shown in Table 2.

Histopathologic features: Microscopic sections of the right and left mammary gland regions in the control negative showed normal histologic features as in (Fig. 1a-c and 2a, b) respectively. The mammary gland composes of lobules of secretory acini with the ductal system (terminal lobular duct and large duct) that is surrounded by stroma. The acini were lined by a single layer of dark cells with myoepithelial cells. Normal ducts had a three-layer structure that comprised ductal epithelial cells, myoepithelial cells, and a basement membrane. The interstitial tissues were mostly composed of fatty tissues.

Histopathological analyses revealed that the mammary tumors were very heterogeneous, the eighty-seven tumors were induced by DMBA and classified into several types with different percentages as shown in Fig. 2; Lobular carcinoma in situ (LCIS), maximum number 8 (6.96. %) was developed in the left side vs. to the right 5 (4.35%), invasive ductal carcinoma (DCIS) in left regions showed greatest value 27 (23.49%) in comparison to the right area 13 (11.31%), fibroadenoma only found in the right side of the mammary gland 11 (9.57%) and invasive lobular carcinoma was developed in the left side by the large number 14 (12.18%) vs. to the right side that showed lesser in number 9 (7.8%) (Fig. 2).

Table 1: The Locations and numbers of mammary tumors in both regions of the rat's mammary gland.

Locations	Rt	Lt	Bilateral	Total (%)	P- Value
Cervico-thoracic	21 (44%)	23 (48%)	3 (8%)	47 (54.02%)	0.9944
Inguino-abdominal	18 (45%)	20 (50%)	2 (5%)	40 (45.98%)	
Total (%)	39 (44.83%)	43 (49.43%)	5 (5.75%)	87	

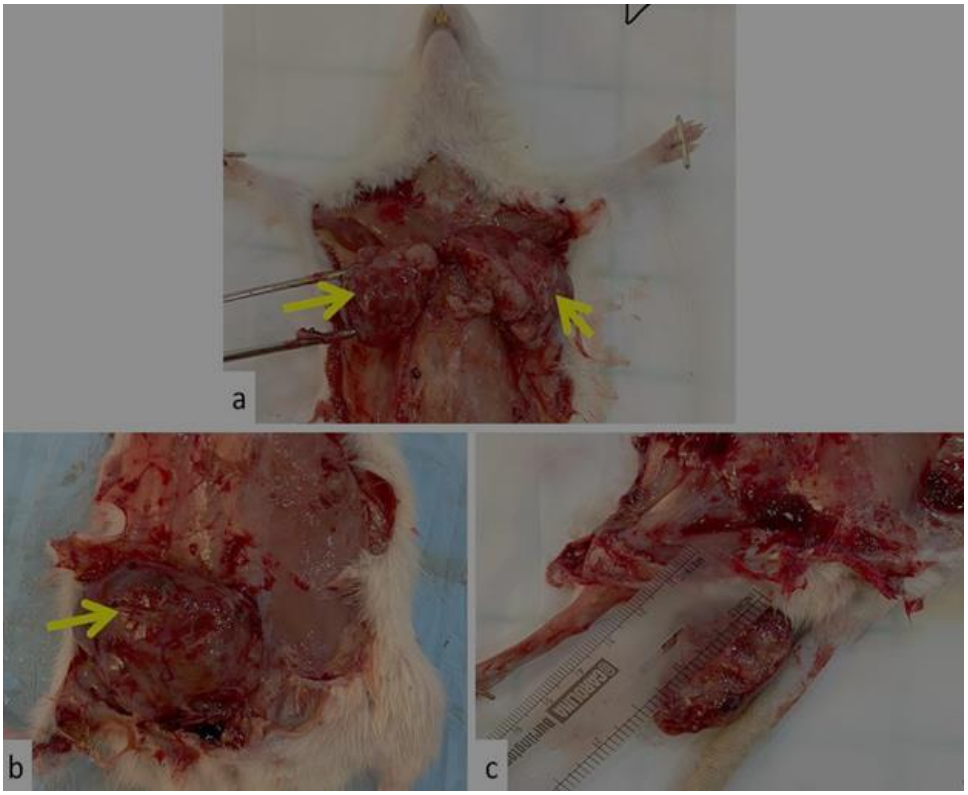

Fig. 1: Gross lesion of rat's mammary gland in right and left flank regions showed; a: Large irregular lumPabout 2-3 cm raised from the flank region on both sides. b: Large irregular white-pink firm lobulated mass that is freely movable in the subcutis raised from the right mammary gland. c: Discoid mass measured by vernier caliper with consistency rubbery.

Table 2: Measurement of tumor size (cm) and weight (gm) in two regions on the Right and Left rat's mammary gland.

Tumor's location	Rt (mm)	Lt (mm)	P-Value
Cervicothoracic	23.45±0.9542	20.48 ± 0.8623	0.023
	2.272 ± 0.08481	1.969 ± 0.08346	0.013
Inguinoabdominal	25.51 ± 0.8616**	22.49 ± 0.8355**	0.021
	2.576 ± 0.1288*	2.186 ± 0.1226**	0.031
All	25.66 ± 0.8421**	22.22 ± 0.8206**	0.004
	2.408 ± 0.07600**	2.067 ± 0.07245**	0.001

Values are Mean±SE, each first row for the size of the tumor and the second row for the weight of the tumor. An unpaired T-test was used for the statistical analysis and **P<0.05.

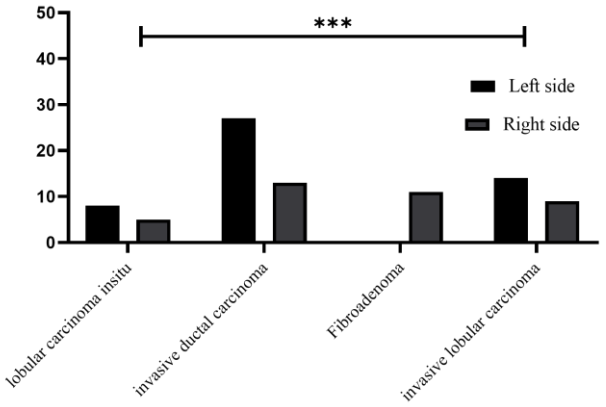

Fig. 2: The chart showed different types of mammary tumors induced by DMBA in both the right and left regions of the rat's mammary gland.

When examined under the microscope, the lobular carcinoma in situ (LCIS) in both locations was seen to have the monomorphic, dyshesive proliferation of monotonous cells, round-oval nuclei in the cell's center, regular nuclear membranes, uniform chromatin, and sparse cytoplasm without mitotic division. Proliferating cells are organized in a glandular pattern with an eosinophilic material-containing cystic dilatation in the center of each cell (Fig. 3d and Fig. 4c,d).

The majority of the pathologic characteristics of fibroadenomas are papillary-cystic growth patterns that result in adenosis and duct papillomatosis. These dilated ducts are filled with papillary ingrowths (dark purple), and only the right region of the mammary gland can identify eosinophilic material within these ingrowths (Fig. 3e-g).

Invasive ductal carcinoma (DCIS) histological investigation indicated strong epithelial cell growth in a distended duct that was divided by secondary lumina with central necrosis. Highly pleomorphic cuboidal to oval cells with protruding nucleoli and spherical, vesicular nuclei can take on a variety of morphologies, such as varying cyst sizes, or be grouped to create regular cribriform gaps (Fig. 3 h- j and Fig. 4 e- j).

Invasive lobular carcinoma's microscopic characteristics showed that the tumor cells are tightly packed in small clusters, forming a pattern of thin strands of cells arranged linearly (Indian file), and the tumor cells may be dispersed irregularly in a densely fibrotic stroma, which is seen diffusely infiltrating breast tissue and fat (Fig. 3 k, I and Fig. 4k, i).

Immunohistochemistry analysis: For all markers, the mammary gland in the control negative sections showed no

Table 3: The scoring system and percentages for all positive antibody markers staining among different types of tumors.

Tumors types	ER	PR	HER2	Ki-67
LCIS	(score 1, 10%)	(score 8, 78%)	(score 4, 35%)	(score 8, 70%)
DCIS	(score 6, 48%)	(score 12, 85%)	(score 4, 35%)	(score 8, 70%)
Invasive lobular carcinoma	(score 8, 75%)	(score 8, 75%)	(score 0)	(score 0)

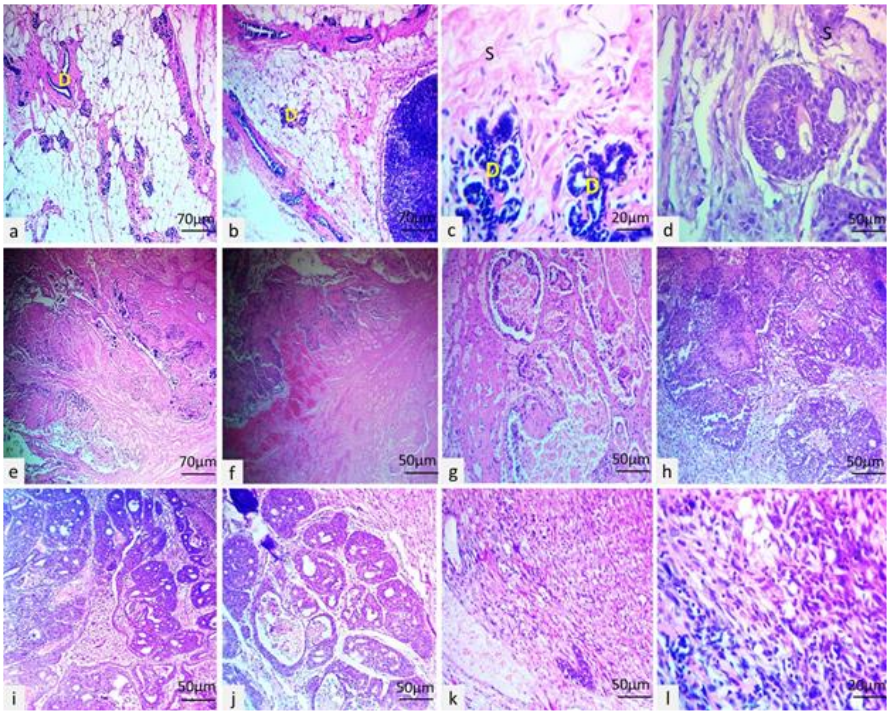

Fig. 3: Microscopic section of the right mammary gland in rat showed; a-c: Normal histologic structure of mammary nodule, terminal ductule (D), and stroma (S) with fatty tissue. d: Lobular carcinoma in situ (LCIS), proliferated cells forming an adenoid shape that contains microcystic eosinophilic secretion within the lumen. e-g: Neoplastic cells proliferated and formed large tubule-cystic that have abundant pale eosinophilic (hyaline) secretory material in their lumen with calcification and abundant stroma, fibroadenoma. h-j: Invasive ductal carcinoma (DCIS) with a tubular and cystic shape that is filled with necrotic debris or eosinophilic secretion within the lumen of the proliferated cells with secondary lumina. K and l: Invasive lobular carcinoma showed tumor cells arranged in single files or cords that diffused throughout mammary tissue, (H&E stain).

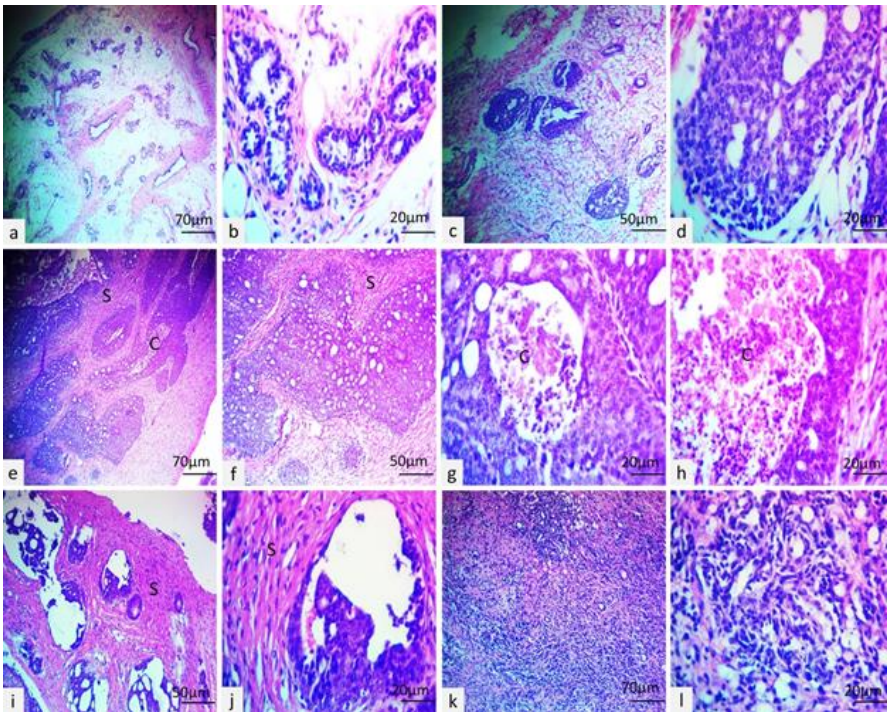

Fig. 4: Microscopic section of the left mammary gland in rat revealed; a and b: Normal histologic morphology of mammary gland nodule, terminal ductule (D), and stroma (S) with fatty tissue and musculature. c and d: Lobular carcinoma in situ (LCIS), neoplastic cells forming an adenoid structure that contains microcystic eosinophilic secretion. e-h: Invasive ductal carcinoma (DCIS), the solid proliferation of pleomorphic cuboidal to oval cells with abundant eosinophilic granular cytoplasm, round vesicular nuclei, and prominent nucleoli in a distended duct with central comedo necrosis (C), which formed a cribriform (C). I and j: Invasive ductal carcinoma (DCIS) with predominantly papillary and partly clinging type manner or cribriform structure with secondary lumina formation. K and l: Invasive lobular carcinoma showed tumor cells arranged in slender strands and cords are seen diffusely infiltrating mammary parenchyma, (H&E stain).

staining (score 0) as in (Fig. 5 a, e, h, k). Regarding the ER marker showed a variable level of nuclear expression and stain intensity according to different types of tumors, as shown in Table 3, weak expression (score 1, 10%) was found in the LCIS vs. to the DCIS that revealed focal-strong positive staining (score 6, 48%) (Fig. 5b,c), while the invasive lobular carcinoma showed diffuse-moderate expression for both ER and PR antibodies markers (score 8, 75%) (Fig. 5d). The brownish nuclear staining for the PR marker was expressed by moderate-diffuse staining (score 8, 78%) in the LCIS vs. to the DCIS that highly expressed and showed diffuse - strong PR staining (score 12, 85%) (Fig. 5f, g). Ki-67 was expressed in the nuclei of neoplastic cells by moderate-diffuse staining (score 8, 70%) in the LCIS and DCIS (Fig. 5i, j). Focal-moderate staining (score 4, 35%) in the LCIS and DCIS was seen for the membranous HER2 expression (Fig. 5l, m). While in the invasive lobular carcinoma, Ki-67 and HER2 showed no stain (score 0) as in Fig. 5n.

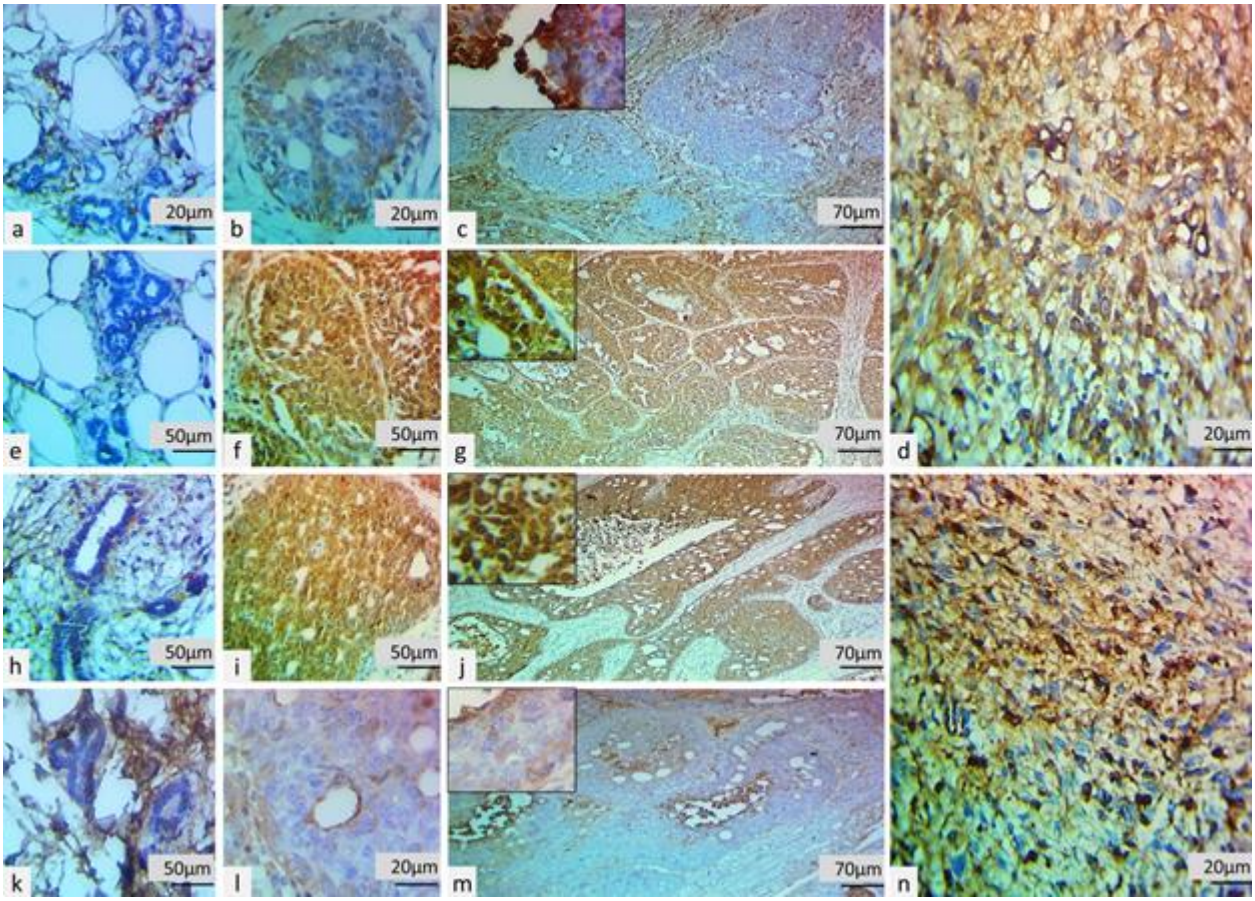

Fig. 5: Immunohistochemical staining of ER, PR, Ki-67, and HER2 nuclear-membranous immunostaining of right and left flank region of rat's mammary gland. a: No ER staining was present (score 0) in the control negative group. b: Weak ER staining (score 1) in the LCIS. c: Focal-strong ER staining (score 6) in the DCIS. d: Diffuse moderate ER and PR staining (score 8) in the invasive lobular carcinoma. e: No PR staining (score 0) in the control negative group. f: Moderate-diffuse PR staining (score 8) in the LCIS. g: Diffuse-strong PR staining (score 12) in the DCIS. h: No Ki-67 staining (score 0) in the control negative group. i: Moderate-diffuse Ki-67 staining (score 8) in the LCIS. j: Moderate-diffuse Ki-67 staining (score 8) in the DCIS. k: No HER2 staining (score 0) in the control negative group. l: Moderate-focal HER2 staining (score 4) in the LCIS. m: Moderate-focal HER2 staining (score 4) in the DCIS n: No Ki-67 and HER2 staining (score 0) in the invasive lobular carcinoma.

DISCUSSION

Mammary cancer is a complex, multistePprocess that can be brought on by chemicals, radiation, viruses, or hereditary factors, according to studies involving experimental animal models. Because rodent cells have less effective DNA repair, poorer genetic stability management, and altered control of gene expression through mechanisms like DNA methylation, they are significantly more susceptible to being converted by chemical carcinogens (Kim *et al*., 2003).

Our study used the DMBA-induced mammary carcinoma model to examine the variation in morpho-histochemical assessment of DMBA-induced mammary cancer in rats, in agreement with a previous study (Lu *et al*., 2006). We demonstrated that the maximum number of tumors developed in the cervicothoracic regions was 47 (45.02%) vs. the inguinoabdominal area, which was 40 (45.98%). Our study is the first document to prove the difference in tumor development regarding the regions of a rat's mammary gland (right and left-sided). The anatomical pattern of rat mammary gland development on the ventral side is attributed to our interpretation of the findings described here regarding the location. The terminal end buds (TEB) first appear when the mammary gland grows, subsequently developing into alveolar buds (AB), and lastly into terminal ducts (TD) at ages around 40 and 60 days (Russo *et al*., 1990), this development progresses differently depending on the gland's anatomical location, which explains why tumor prevalence varies by site. In the anterior locations, such as the cervix and thorax, the transition from TEB to TDs and AB occurs more slowly than in the abdominal and inguinal areas (Anderson *et al*., 2000), this is the reason why in our data the number of tumors increased in the cervicothoracic areas compared to the inguinoabdominal because at this age there are still a significant number of TEB in the cervicothoracic areas have changed into tumors following DMBA induction (Anderson *et al*., 2000). In agreement with our data the previous report documented that when virgin animals are exposed to the carcinogen, glands in the thoracic region grow more cancers than glands in the abdominal-inguinal region. The asynchronous development of the thoracic mammary glands, which hold onto the undifferentiated TEBs for a longer period than mammary glands in different topographic locations, is thought to be the cause of these topographic disparities in tumor incidence (Russo and Russo, 1996).

Our study contradicts the results of a previous investigation conducted by Saminathan *et al*. (2014). regarding the location of tumor growth in mammary glands. According to their findings, 81.82% of tumors (36

out of 44) were detected in the abdominal inguinal glands, and 18.18% (8 out of 44) were found in cervical thoracic gland pairs. Interestingly, they also observed that tumor development occurred 4.8 times more frequently in cervical thoracic pairs than in abdominal-inguinal pairings. Furthermore, Mayilkumar and Pawaiya (2009) observed that tumor development occurs 6.3 times more frequently in abdominal-inguinal pairings than in cervico-thoracic pairs. However, our research found a different pattern, as we detected tumors more frequently in cervicothoracic mammary glands than in abdominal inguinal glands.

In the current study, it was observed that the left mammary gland chain had a higher tumor incidence than the right side, although the difference was not statistically significant ($P>0.05$). Furthermore, the tumors located in the inguinoabdominal region (on both sides) were found to be significantly larger and heavier than those in the cervicothoracic region ($P<0.05$). Specifically, the tumors on the right side of both regions were significantly larger and heavier compared to those on the left side ($P<0.05$). These findings were in agreement with the previous observations of Mayilkumar and Pawaiya (2009) reported that the incidence was more in the left mammary chain when compared to the right (Mayilkumar and Pawaiya, 2009). While our findings are in contrast to earlier research, which found no discernible difference between the left and right mammary chains in the emergence of mammary cancers (Saminathan *et al*., 2014).

Through the treatment of DMBA, which mimics the comparable pathway shown in human breast cancer, mammary cancer was developed in the Sprague-Dawley rats used in this work. Additionally, earlier research has shown that the histology, hyperplastic development with premalignant and malignant lesions, and the incidence of human breast cancer are quite similar (Xin and Shang, 2022).

In this study, we found a significant difference between the tumor development after a single dose of DMBA, as demonstrated by the following: the highest number of LCIS, 8 (6.66%), developed on the left side compared to the right, which only had 5 (4.35%); the highest number of DCIS, 27 (23.49%) and the lowest number, 13 (11.31%); the only location of fibroadenoma in the mammary glands, which only occurred on the right side, and a greater proportion of 14 (12.18%) cases of invasive lobular carcinoma were found on the left side compared to 9 (7.8%) cases on the right. The findings of this study differ from those published by Al-Dhaheri *et al*., 2008, who documented that the rats who were given DMBA intraperitoneally developed only ductal and lobular cancer in situ in the mammary glands. Our results agree with earlier research that employed the carcinogen DMBA to induce tumors in the study (Ma *et al*., 2007) which reported intraductal papilloma, fibroadenoma, and adenocarcinoma; additionally, in studies identical to ours, these tumors were only generated by a single oral dose of DMBA (Lee *et al*., 2008). Our findings show a wide range of morphologic changes in fibroadenoma, including hyalinization and calcification. The study by Terada *et al*. (1995), in contrast to our findings, only discovered invasive ductal carcinoma at 20 weeks postpartum. Wistar inbred rats that were weaned on the ninth puerperal day had one mammary gland intraductally injected with 7,12-dimethylbenze (a) anthracene (DMBA) to specifically induce ductal carcinoma; this is why other types of mammary cancer did not develoPbecause epithelioglandular cells in the ducts and terminal ducts had degenerated and detached (Terada *et al*., 1995).

In our study, we used a rat model to induce mammary gland tumors, we observed a higher incidence of tumors on the left side compared to the right. This finding is consistent with the incidence of human breast cancer, where the left breast is more commonly affected than the right. Several observational studies have consistently reported a left-to-right incidence ratio of 1.10. (Fatima *et al*., 2013). The best explanation for why the number of tumors on the left side has risen in comparison to the right side is the anatomic variation of mammogenesis, in which the embryonic flanks develoPin the trunk as two broad lateral areas in which the dorsal paraxial mesoderm intermixes with the ventral lateral plate mesoderm (LPM). Along with the venture, they provide new ventral-lateral borders that serve as bilateral platforms for the emergence of mammary lines. Externally, these alleged mammary-producing regions appear to be LR (left-right) symmetrical. It's noteworthy to observe that the development of the mammary line and MRs is slightly advanced on the left side and that the left side seems to have a greater possibility for mammogenesis (Schmidt, 1998).

Numerous prognostic and predictive indicators have been developed to predict tumor activity in light of the variety of breast cancer. A prognostic biomarker provides data on how a patient will respond to therapy. An extremely significant predictive biomarker is the expression of ER and/or PR (Siddarth *et al*., 2016). In the present study, we analyzed some tumor markers in DMBA-induced rat mammary tumors by immunohistochemistry. In this study, the mammary gland section in the control negative for all antibody markers showed negative results (score 0). Regarding the ER marker, it showed the variable level of nuclear expression and stain intensity according to different types of tumors; weak expression (10%) was found in the LCIS vs. to the DCIS that revealed focal-strong positive staining (48%), while the invasive lobular carcinoma showed diffuse-moderate expression for both ER and PR genes (75%), in agreement with our data from the Ma *et al*. (2007) experiments, ER-positive showed in all tumors induced by DMBA including; intraductal papilloma, fibroadenoma, and adenocarcinoma. According to earlier studies, mammary tumors in rats continue to express ER and PR, and the percentage of ER-positive cells fluctuates from 15.1% to 57.5% (Ross, 2015). In our results, the brownish nuclear staining of the PR antibody marker was expressed by moderate-diffuse staining (78%) in the LCIS vs. to the DCIS that was highly expressed by diffuse-strong PR staining (85%), this finding is comparable to the earlier research, which described a DMBA-induced mammary tumor with a strong positive intensity for the markers ER and PR (Abba *et al*., 2016). Similar to the human study, invasive breast cancer is shown to have more than 60-70% positive cells for the ER and PR receptors (Nabi *et al*., 2016). Contrary to our findings, the study revealed that the frequency of ER and PR expressions was between 40% and 60% respectively (Fidianingsih *et al*., 2022). An ER expression frequency of 39.89% and a PR expression ratio of 21.56% were seen after DMBA induction (Alvarado *et al*., 2017). In past studies on

humans, invasive ductal carcinomas with ER and PR expression were observed in 60-80% of cases and 60–70% of cases, respectively. This level of expression for both markers is comparable to our work on the expression of ER and PR in ductal invasive carcinoma (Patnayak *et al*., 2015). That after ductal carcinoma, lobular carcinoma is the most prevalent kind of breast cancer, in the study (Lakhani *et al*., 2012), sixty-seventy percent of lobular carcinomas are ER positive. Although this tumor has a good prognosis, it is linked to a worse long-term result than ductal carcinoma due to greater rates of mortality, recurrence, and distant metastases.

Ki 67 is a cell cycle and proliferation marker. The c-myc activity led to the onset of the cell cycle. C-myc, cyclin D1, and aryl hydrocarbon receptor expressions are all increased by DMBA induction (Currier *et al*., 2005). This study demonstrated a high Ki67 expression in the LCIS and DCIS by moderate-diffuse staining (70%). While in the invasive lobular carcinoma, Ki-67 and HER2 showed no stain. Our results are consistent with all of the referenced studies that reported high Ki67 (60-80%) expressions (Boder *et al*., 2013; Aiad *et al*., 2014). Patient outcomes, such as disease-free survival or survival rates, have a substantial correlation with the likelihood of relapse in breast cancers that overexpress Ki-67 in more than 20-50% of the cells (Assersohn *et al*., 2003). Elevated-grade tumors, advanced age, lymph node metastases, and other poor prognostic clinicopathological characteristics were found to be substantially related to this high expression of Ki67. We did not uncover any lymph node metastases, which is consistent not only with our findings but also with the results of many earlier investigations (Pathmanathan *et al*., 2014), concerning the predictive and prognostic significance of Ki-67 expression levels in the emergence of breast cancer, this demonstrates the scientific premise that malignant neoplasms lose their ability to discriminate when tumor cells multiply rapidly (Pathmanathan and Balleine, 2013). Similar to our study the majority of invasive lobular carcinomas (ILCs) typically do not express Ki-67 and showed no stain (score 0) (Boukhechba *et al*., 2018). Previous studies using 10 mg/100 g/BW-induced rats revealed poor Ki-67 expressions (35.5%) (Zhao *et al*., 2011).

HER2 has been successfully targeted in the treatment of breast cancer, and its potential as a therapeutic target is being researched (Iqbal and Iqbal, 2014). In our study, a high amount of membranous HER2 expression was found by focal-moderate staining (35%) in the LCIS and DCIS, but no expression was seen in the invasive lobular carcinoma. According to a previous report, invasive ductal carcinoma had significant HER2 expression (Singh *et al*., 2019). Similar to our study the majority of invasive lobular carcinomas (ILCs) typically do not express HER2 and showed no stain (score 0) (Boukhechba *et al*., 2018). HER2 overexpression was observed in the cases reported by Cserni *et al*. (2010) and Yu *et al*. (2017) which is in contrast to our finding.

Conclusions: The incidence of tumors on the left side is more than the left side induced in the rat by DMBA and its development varies according to the mammary gland region. The tumor mass on the right side was greater and heavier vs. the left side. Our carcinogenesis model developed new types of tumors that were not reported by the other study including invasive lobular carcinoma by the single oral dose at week 16. The expression of all prognostic markers ER, PR, Ki-67, and HER2 had a good characteristic similar to human breast cancer.

Acknowledgments: We would like to express our sincere gratitude to the College of Medicine and Animal House at Hawler Medical University in Hawler, Iraq for their invaluable support and maintenance. Our sincere thanks also go to the Ministry of Higher Education and Scientific Research, Kurdistan Regional Government, Kurdistan, Iraq for funding this project. This collaboration has been a key factor in our success and we are deeply appreciative of the support provided.

Conflict of interest: All authors declare no conflict of interest.

Authors contribution: The experiment in this study was performed by Nali A. Maaruf, Suhel M. Najjar and Salah A. Ali. Suhel M. Najjar and Salah A. Ali provided supervision, developed the initial concept, and co-wrote the article, ensuring the accuracy of the data. Nali A. Maaruf, Suhel M. Najjar, and Salah A. Ali also wrote the paper. Snur M.A. Hassan had a crucial role in pathological section interpretation and data analysis.

REFERENCES

Abba MC, Zhong Y, Lee J, *et al*., 2016. DMBA-induced mouse mammary tumors display a high incidence of activating Pik3caH1047 and loss of function Pten mutations. Oncotarget 7:64289-99.

Aiad HA, Samaka RM, Asaad Ny, *et al*., 2014. RelationshiPof CK8/18 expression pattern to breast cancer immunohistochemical subtyping in Egyptian patients. Ecancermedicalscience 8:400-4.

Akkaya ÖÖ, Nawaz S, Dikmen T, *et al.,* 2022. Determining the Notch1 Expression in Chondrogenically Differentiated Rat Amniotic Fluid Stem Cells in Alginate Beads Using Conditioned Media from Chondrocytes Culture. Biol Bull Russ Acad 49(Suppl 3):9-20.

Al-Dhaheri WS, Hassouna I, Al-Salam, *et al*., 2008. Characterization of breast cancer progression in the rat. Ann NY Acad Sci 1138:121-31.

Alvarado A, Lopes AC, Faustino-Rocha AI, *et al*., 2017. Prognostic factors in MNU and DMBA-induced mammary tumors in female rats. Pathol Res Pract 213:441-6.

Anderson L, Morris J, Sasser L, *et al*., 2000. Effect of constant light on DMBA mammary tumorigenesis in rats. Cancer Lett 148:121-126.

Asif HM, Sultana S, Akhtar N, *et al*., 2014. Prevalence, risk factors and disease knowledge of breast cancer in Pakistan. Asian Pac J Cancer Prev 15:4411-6.

Assersohn L, Salter J, Powles T, *et al*., 2003. Studies of the potential utility of Ki67 as a predictive molecular marker of clinical response in primary breast cancer. Breast Cancer Res Treat 82:113-23.

Al-Nuaimi HA-A, Hamdi E and Mohammed BB, 2020. Ki-67 Expression in Breast Cancer, Its Correlation with ER, PR and Other Prognostic Factors in Nineveh Province. Annals of the College of Medicine, Mosul 42:1-10.

Barros ACS, Muranaka ENK, Mori LJ, *et al*., 2004. Induction of experimental mammary carcinogenesis in rats with 7, 12-dimethylbenz (a) anthracene. Revista do Hospital das Clínicas 59:257-61.

Boder J, Abdalla F and Elfagieh M, 2013. Proliferative activity in Libyan breast cancer with comparison to European and central African patients. Biomed Res Int: 831714.

Boukhechba M, Kadiri H and El Khannoussi B, 2018. Invasive lobular carcinoma of the breast with extracellular mucin: case report of a new variant of lobular carcinoma of the breast. Case Reports Pathol 2018:1-3.

Bülbül T and Nawaz S, 2020. An overview of Laboratory Rodents, Digestive Physiology and Important Issues regarding Their Nutrition. Osmaniye Korkut Ata Üniv 3:219-27.

Cheng A, Liang Z, Liang L, *et al*., 2018. Breast cancer laterality and molecular subtype likely share a common risk factor. Cancer Manag Res 10:6549.

Cheung C, Loy S, Li GX, *et al*., 2011. Rapid induction of colon carcinogenesis in CYP1A-humanized mice by 2-amino-1-methyl-6-phenylimidazo [4, 5-b] pyridine and dextran sodium sulfate. Carcinogenesis 32:233-9.

Cserni G, Floris G, Koufopoulos N, *et al*., 2017. Invasive lobular carcinoma with extracellular mucin production-a novel pattern of lobular carcinomas of the breast. Clinico-pathological description of eight cases. Virchows Arch 471:3-12.

Currier N, Solomon SE, Demicco EG, *et al*, 2005. Oncogenic signaling pathways activated in DMBA-induced mouse mammary tumors. Toxicol Pathol 33:726-37.

Davey M, Hynes S, Kerin, *et al*., 2021. Ki-67 as a prognostic biomarker in invasive breast cancer. Cancers 13:4455.

De Oliveira KD, Avanzo GU, Tedardi MV, *et al*., 2015. Chemical carcinogenesis by DMBA (7, 12-dimethylbenzanthracene) in female BALB/c mice: new facts. Braz J Vet Res Anim Sci 52:125-33.

Dong F, Shen Y, Xu T, *et al*., 2018. Effectiveness of urine fibronectin as a non-invasive diagnostic biomarker in bladder cancer patients: a systematic review and meta-analysis. World J Surg Oncol 16:50-61.

Fatima N, Zaman MU, Maqbool A, *et al*., 2013. Lower incidence but more aggressive behavior of right sided breast cancer in Pakistani women: does right deserve more respect? Asian Pac J Cancer Prev 14:43-5.

Fidianingsih I, Aryandono T, Widyarini S, *et al*., 2022. Profile of Histopathological Type and Molecular Subtypes of Mammary Cancer of DMBA-induced Rat and its Relevancy to Human Breast Cancer. Open Access Maced J Med Sci 10:71-8.

Hassan SMA, Saeed AK, Rahim OO, *et al*., 2022. Alleviation of cisplatin-induced hepatotoxicity and nephrotoxicity by L-carnitine. Iranian J of Basic Medi Sci 25:890-7.

Iqbal N and Iqbal N, 2014. Human epidermal growth factor receptor 2 (HER2) in cancers: overexpression and therapeutic implications. Mol Biol Int 2014:1-9.

Kim J B, O'Hare MJ and Stein R, 2003. Models of breast cancer: is merging human and animal models the future? Breast Cancer Res 6:22-30.

Lakhani SR, Ellis IO, Schnitt S, *et al*., 2012. WHO Classification of Tumours of the Breast 4:978-92

Lee H-J, Lee YJ, Kang CM, *et al*., 2008. Differential gene signatures in rat mammary tumors induced by DMBA and those induced by fractionated γ radiation. Radiation Research 170:579-90.

Lu S, Shen K, Wang Y, *et al*., 2006. Atm-haploinsufficiency enhances susceptibility to carcinogen-induced mammary tumors. J. Carcinog 27:848-55.

Mayilkumar K and Pawaiya R, 2009. Evaluation of C-erbB2 and Estrogen Receptor Expression in Chemically Induced Rat Mammary Tumours. Indian J Vet Pathol 2:242-4.

Meng X, Song S, Jiang Z F, *et al*., 2016. Receptor conversion in metastatic breast cancer: a prognosticator of survival. Oncotarget 7:71887-903.

Nabi MG, Ahangar A and Kaneez S, 2016. Estrogen receptors, progesterone receptors and their correlation concerning HER-2/neu status, histological grade, size of the lesion, lymph node metastasis, lymphovascular involvement and age in breast cancer patients in a hospital in north India. Asian J Med Sci 7:28-34.

Nawaz S, 2020. TGFβ-3/IGF-1 ilave edilmiş kondrosit kaynaklı koşullandırılmış medyumun amniyotık sıvı kaynaklı hücrelerde kondrogenezis üzerine etkileri. http://acikerisim.aku.edu.tr/xmlui/handle/11630/8398

Pathmanathan N and Balleine RL, 2013. Ki67 and proliferation in breast cancer. J Clin Pathol 66:512-6.

Pathmanathan N, Balleine RL, Jayasinghe UW, *et al*., 2014. The prognostic value of Ki67 in systemically untreated patients with node-negative breast cancer. J Clin Pathol 67:222-8.

Patnayak R, Jena A, Rukmangadha N, *et al*., 2015. Hormone receptor status (estrogen receptor, progesterone receptor), human epidermal growth factor-2 and p53 in South Indian breast cancer patients: A tertiary care center experience. Indian J Med Paediatr Oncol 36:117-22.

Russo, J., 2015. Significance of rat mammary tumors for human risk assessment. Toxicol Pathol, 43:145-70.

Russo IH and Russo J, 1996. Mammary gland neoplasia in long-term rodent studies. Environ Health Perspect 104:938-67.

Russo J, Gusterson BA, Rogers AE, *et al*., 1990. Comparative study of human and rat mammary tumorigenesis. Lab Invest 62:244-78.

Saminathan M, Rai R, Dhama K, *et al*., 2014. Histopathology and immunohistochemical expression of N-Methyl-N-Nitrosourea (NMU) induced mammary tumors in Sprague-Dawley rats. Asian J Anim Vet Adv 9:621-40.

Schmidt H, 1998. Supernumerary nipples: prevalence, size, sex, and side predilection–a prospective clinical study. Eur J Pediatr 157:821-823.

Shah RJ, Kothari S and Patel S, 2016. Correlation of Her-2/neu status with estrogen, progesterone receptors and histologic features in breast carcinoma. Annals of Pathol and Lab Med 3:476-83.

Siddarth BR, Kumar A, Kumar S, *et al*., 2016. A clinicopathologic study of infiltrating carcinoma of breast and correlation with the ER/PR status. J Evol Med Dent Sci 5:1025-33.

Singh M, Kumar J, Omhare A, *et al*., 2019. Study on Histopathological Correlation with ER, PR, and HER 2 Neu Receptor Status in Breast Carcinoma and its Prognostic Importance. SSR Inst Int J Life Sci 5:2130-6.

Sung H, Ferlay J, Siegel RL, *et al*., 2021. Global cancer statistics 2020: GLOBOCAN estimates of incidence and mortality worldwide for 36 cancers in 185 countries. CA: a Cancer J Clinic 71:209-49.

Taneja, P, Maglic D, Kai F, *et al*., 2010. Classical and novel prognostic markers for breast cancer and their clinical significance. Clin Med Insights Oncol 4:4773.

Terada S, Uchide K, Suzuki N, Akasofu K, *et al*., 1995. Induction of ductal carcinomas by intraductal administration of 7, 12-dimethylbenz (a) anthracene in Wistar rats. Breast Cancer Res Treat 1:35-43.

Vedashree M and Rajalakshmi V, 2016. Clinico-pathological study of breast carcinoma with correlation to hormone receptor status & HER2/neu. Indian J Pathol Oncol 3:690-5.

Wincewicz A, Baltaziak M, Kanczuga-Koda L, *et al*., 2010. Aberrant Distributions and Relationships Among E-cadherin, β-catenin and Connexin 26 and 43 in Endometrioid Adenocarcinomas. Int J Gynecol Pathol 29:358-65.

Xin J and Shang Y, 2022. Alternariol alleviates breast carcinoma by inhibiting cellular proliferation correlated with increased apoptotic events in rats. Eur J Inflamm 7:1-13.

Yu J, Bhargava R and Dabbs DJ, 2010. Invasive lobular carcinoma with extracellular mucin production and HER-2 overexpression: a case report and further case studies. Diagn Pathol 5:1-7.

Zhao J-A, Chen JJ, Ju YC, *et al*., 2011. The effect of childbirth on carcinogenesis of DMBA-induced breast cancer in female SD rats. Chin J Cancer 30:779-85.